# Diffraction-free acoustic detection for optoacoustic depth profiling of tissue using an optically transparent polyvinylidene fluoride pressure transducer operated in backward and forward mode

**Michael Jaeger**
**Joël J. Niederhauser**
**Marjaneh Hejazi**
**Martin Frenz**
University of Berne
Institute of Applied Physics
Sidlerstrasse 5, CH-3012 Bern
Switzerland
E-mail: frenz@iap.unibe.ch

**Abstract.** An optoacoustic detection method suitable for depth profiling of optical absorption of layered or continuously varying tissue structures is presented. Detection of thermoelastically induced pressure transients allows reconstruction of optical properties of the sample to a depth of several millimeters with a spatial resolution of 24 $\mu$m. Acoustic detection is performed using a specially designed piezoelectric transducer, which is transparent for optical radiation. Thus, ultrasonic signals can be recorded at the same position the tissue is illuminated. Because the optoacoustical sound source is placed in the pulsed-acoustic near field of the pressure sensor, signal distortions commonly associated with acoustical diffraction are eliminated. Therefore, the acoustic signals mimic exactly the depth profile of the absorbed energy. This is illustrated by imaging the absorption profile of a two-layered sample with different absorption coefficients, and of a dye distribution while diffusing into a gelatin phantom.  [DOI: 10.1117/1.1891443]

Keywords: photoacoustics; pressure transducer; signal detection; stress analysis; acoustic diffraction; medical imaging.

Paper 04065 received May 4, 2004; revised manuscript received Sep. 10, 2004; accepted for publication Nov. 1, 2004; published online Apr. 14, 2005.

## 1 Introduction

In medicine, there is a need for noninvasive real-time monitoring of skin tissue, i.e., its layered structure, blood perfusion, or pathological abnormalities. Besides, diffusion properties of topically applied drugs are of major interest. Medical optoacoustics (OA), based on the generation of sound due to absorption of light, combines the advantages of ultrasound and optics, and opens new perspectives in noninvasive diagnostics and monitoring of subsurface tissue layers. Acoustical waves are generated directly inside the tissue due to absorption of short laser pulses. Rapid local heating of the tissue leads to a sudden pressure rise proportional to the volumetric absorbed energy density. After heating, the resulting nonuniform pressure distribution propagates toward the surface, where it can be measured spatially and temporally resolved with an acoustic receiver. From the obtained pressure signals, the original distribution of absorbed energy density can then be recalculated using the relation between acoustic propagation time and distance. This method is suited for measuring spatial resolved optical tissue properties (absorption, scattering), and for imaging absorbing structures to a depth of several millimeters or even centimeters.

Address all correspondence to Martin Frenz. Institute of Applied Physics, Biomedical Photonics, Univ. Bern, Sidlerstrasse 5, Bern, Switzerland CH-3012 Switzerland. Tel: 41 31 631 9043; Fax: 41 31 6313 765; E-mail: frenz@iap.unibe.ch

In recent years, much effort in development of ultrasound detection methods, including piezoelectric detection[1,2] and optical detection[3–15] on one hand, and of image reconstruction methods[11,14,16–18] on the other hand, has led to quite sophisticated systems for 2- or 3-D imaging of tissue and tissue phantoms.[18,19] However, most of these methods show mere qualitative results in the sense that they focus on using tissue optical properties for imaging contrast and not on calculating them quantitatively.

Sensitivity and resolution of acoustic detection partly contradict each other, and in the field of quantitative OA measurements, mostly a single sensor with low spatial resolution but high sensitivity was used for measurements of layered samples, like skin tissue.[2,7,10,20,21] The OA signal was considered a copy of an absorption depth profile that is distorted by acoustic diffraction due to the finite lateral extent of the illuminated sample region.[20,22] The drawback of a single pressure sensor is that the interpretation of the measured signal is only unambiguous if the actual light distribution is exactly known, which in a highly scattering sample like skin tissue is *a priori* not the case.

In this study we introduce a new approach to quantitative OA, in which the effect of acoustic diffraction is eliminated. Since source and receiver are in linear wave dynamics equivalent by inversion of time, an acoustic near field can be as-

1083-3668/2005/$22.00 © 2005 SPIE

signed to the transducer. In the acoustic near field, the measured pressure transients exactly mimic the shape of the original pressure distribution, and consequently replicate the depth profile of absorbed laser energy in the irradiated tissue sample. This allows reconstruction of the optical properties of layered samples without the need of basic assumptions about the light distribution inside the sample.

For the measurements, we designed a transducer that uses a transparent piezoelectric polyvinylidene fluoride (PVDF) film, together with salt-water cavities instead of opaque metal coatings as electrodes; thus detection can easily be done in reflection mode (sample is irradiated over the surface where OA signals are detected). Placing the sample in the transient acoustics near field of this transducer, we measure depth-dependent absorption coefficients in layered structures and time-resolved diffusion of dyes into tissue phantoms.

## 2 Theory of Diffraction-Free Optoacoustic Detection

Illumination of a tissue sample with a short laser pulse leads (due to fast heating) to the generation of a pressure transient in the absorbing region. The absorbed energy is distributed in the illuminated volume as energy density $u(\mathbf{x}')\,[\mathrm{J\,m^{-3}}]$, which depends on the absorption coefficient $\mu_a\,[\mathrm{m^{-1}}]$ and on the fluence $\Phi\,[\mathrm{J\,m^{-2}}]$.

$$u(\mathbf{x}')=\mu_a(\mathbf{x}')\cdot\Phi(\mathbf{x}'). \tag{1}$$

If the irradiation time is much shorter than the sound transition time through the illuminated volume (stress confinement), heating of the tissue leads to a pressure rise $\Delta p(\mathbf{x}')\,[\mathrm{Pa}]$ that is correlated to $u(\mathbf{x}')$ by the Grüneisen parameter $\Gamma$ ($\sim$0.1 Pa$\times$m$^3$/J in water)[21]:

$$\Delta p(\mathbf{x}')=\Gamma(\mathbf{x}')\cdot u(\mathbf{x}'). \tag{2}$$

In consequence, a temporally varying pressure field $p'(\mathbf{x},t)\,[\mathrm{Pa}]$ is generated, with the initial condition $p'(\mathbf{x},t=0)=\Delta p(\mathbf{x}'=\mathbf{x})$.

By measuring the initial pressure distribution $\Delta p(\mathbf{x}')$, the distribution of absorbed energy $u(\mathbf{x}')$ can be determined and optical properties can be derived according to Eq. (1). The initial pressure distribution can be measured indirectly by detecting the sound field $p'(\mathbf{x},t)$ at the sample surface and inversely solving the wave equation. In the case of a layered sample like skin tissue, differences between the optical properties of the various layers are reflected in the depth profile of absorbed energy. Also, the concentration of permeating drugs will characteristically change along the depth axis of the sample and influence the depth profile of absorption. If a depth profile of a layered structure like skin tissue is of interest, the best detection method is one that maps the depth distribution of original pressure onto the time-resolved signal amplitude.

In harmonic continuous acoustics, an ultrasonic receiving element is defined by its angular sensitivity, which also depends on the acoustic wavelength. A receiver that integrates pressure over a plane surface with infinite lateral size is perfectly directional for all acoustic wavelengths, because only harmonic waves with wave vectors parallel to the plane normal are not canceled in detection. Detection with such a receiver would be equivalent to perfect 1-D sound propagation along the sample depth axis, and a perfect mapping of the depth profile onto the signal shape could be observed. In transient acoustics, this situation is possible even with a plane sensor of finite size, because the principle of temporal causality can be applied. This means that the edge of a sensor has no physical importance until the acoustic transient has reached it. Before, the sensor is equivalent to one with infinite lateral size. No distortions due to acoustic diffraction (that belong to the presence of a finite lateral aperture) are noticed in the early part of the signal and the shape of the signal $s(t)$ perfectly mimics the profile of the original pressure distribution along the axis normal to the sensor surface:

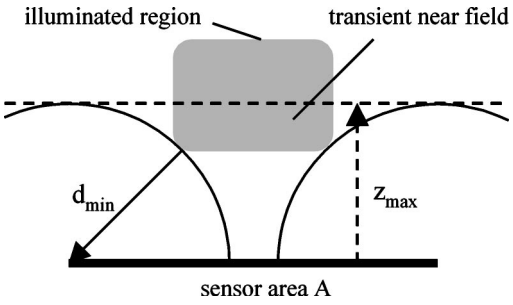


**Fig. 1** A sketch of the sensor-sample geometry is shown. After irradiation at time zero, acoustic transients originating from the edge of the illuminated sample region need to travel the distance $d_{\mathrm{min}}$ to reach the edge of the sensor area. Signals originating from the illuminated region in front of vertical distances less than $z_{\mathrm{max}}=d_{\mathrm{min}}$ are detected prior to the first arrival of any transient at the edge of the sensor area, thus they are detected as if the sensor would have infinite size. Viewed from this region, the sensor seems to be perfectly directional, and the signal is detected as if sound propagation was in direction perpendicular to the sensor surface. As a consequence, the detected signal exactly mimics the depth distribution of initial pressure up to the depth $z_{\mathrm{max}}$.

$$s(t)\propto\int\int \mathrm{d}x\mathrm{d}y \quad \Delta p(x,y,z=vt), \tag{3}$$

where $v$ is the velocity of sound, and $z$ is the distance of a point inside the sample to the sensor surface.

The region from where such undistorted signals can be detected defines the acoustic near field for the ultrasonic sensor. In analog to continuous acoustics, where the near field depends on the acoustic wavelength, the size of the near field in transient acoustics not only depends on the sensor, but also on the sound source geometry. The extent of the original pressure distribution defines the region from where undistorted signals can be detected. This can be derived graphically as depicted in Fig. 1. The lateral extent of the source, defined by irradiation cross section and scattering, has to be smaller than that of the sensor. The transients originating from the edges of the source need some time to travel the minimal distance $d_{\mathrm{min}}$ to the sensor edge. The signal originating from the region between the sample surface and the depth $z_{\mathrm{max}}=d_{\mathrm{min}}$ is detected prior to the arrival of any transient at the sensor edge. This region is in the transient acoustic near field of the detection system, in which real depth profiles can directly be acquired from the shape of the signal.

**Table 1** Acoustic properties of used materials.

| Material | $Z\,[10^6\,\mathrm{kg\,m^{-2}\,s^{-1}}]$ | $v\,[10^3\,\mathrm{ms^{-1}}]$ |
|---|---|---|
| Water | 1.5 | 1.5 |
| Soft tissue | 1.36 to 1.66 | 1.48 to 1.57 |
| PVDF | 4.2 | 2.3 |

These considerations are valid if sound propagation is linear. This means acoustical mismatch on interface,[1,21] causing sound refraction and sound reflection, has to be avoided. In our case, pressure is measured with a piezoelectric foil, embedded in water for acoustic coupling to the tissue surface, since water has acoustic properties close to soft tissue. As can be seen in Table 1, the PVDF of the sensor layer represents a significant impedance step to an incoming pressure wave. Figure 2 shows a typical measurement situation where such a wave with wavelength $\lambda$ hits a sensor layer (thickness $d$) under an incident angle $\varphi_1$. The requirement of continuity of pressure at the interfaces leads, for the case of $\lambda \gg d$, to the conclusion that the sensor layer is acoustically transparent and the amplitude $p_2$ measured inside the sensor is identical with the amplitude $p_3$ transmitted into the backing layer. Therefore, $p_2$ only depends on the acoustic properties of the front and backing material. For this case, the detected amplitude can be calculated using the well-known acoustic transmission formula:

$$\frac{p_2}{p_1}=\frac{p_3}{p_1}=\frac{2Z_3'}{Z_1'+Z_3'}, \quad \text{where} \quad Z_i'=\frac{Z_i}{\cos\varphi_i}, \qquad \sin\frac{\varphi_i}{/v_i}=\sin\frac{\varphi_1}{/v_1}, \tag{4}$$

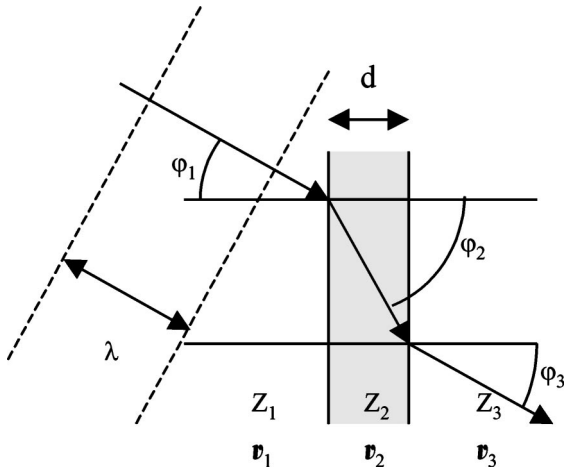


**Fig. 2** Model for wave propagation through the sensor layer. The sensor layer violates the supposition of acoustic homogeneity. Nevertheless, if the sensor thickness $d$ is smaller than the characteristic acoustic wavelength $\lambda$, mainly the front and backing material determine acoustic reflection and transmission. In the special case where the impedances $Z_1$ and $Z_3$ are equal, transmission to the sensor layer is one, and pressure is detected as without acoustic discontinuity.

where $Z_i$, $v_i$, and $\varphi_i$ are acoustic impedance, sound velocity, and propagation angle in the various layers in their succession of sound propagation.

This formula shows that if the acoustic properties of the media before and behind the sensor foil are identical, the detected amplitude $p_2$ is additionally independent of the incident angle and equals to $p_1$, as in the case of linear sound propagation.

Additionally, the signal could be influenced by the excitation of lamb waves in the sensor foil. Bacon[23] discussed the influence of lamb wave excitation on the angular sensitivity, depending on the product of frequency and sensor slab diameter, and reported that above 5 MHz×mm, this influence can be neglected.

## 3 Material and Methods

A piece of piezoelectric polyvinylidene fluoride (PVDF) foil was used for the sensor. Assuming an acoustical wavelength longer than the foil thickness, the total charge $Q\,[\mathrm{C}]$ induced by a pressure $p$ over the thin foil with the area $A$ is:[24]

$$Q(t)=d_{33}\int_A dA \;\; p(\mathbf{x},t), \tag{5}$$

where $A\,[\mathrm{m}^2]$ is the foil area, and $d_{33}\,[\mathrm{C/N}]$ is the piezoelectric charge constant.

Charge conducting covers on both sides of the foil build a capacitor $C$. The open-circuit voltage $U\,[\mathrm{V}]$ over this capacitor equals $Q/C$ and is therefore proportional to the pressure averaged over the foil surface:

$$U(t)=\frac{Q(t)}{C}=\frac{d\cdot d_{33}}{A\cdot\epsilon\epsilon_0}\int_A dA \;\; p(x,t) =d\cdot g_{33}\cdot\frac{1}{A}\int_A dA \;\; p(x,t), \tag{6}$$

where $d$ is the foil thickness; $\epsilon$, $\epsilon_0$ is relative permittivity and permittivity; and $g_{33}$ is the piezoelectric voltage constant, which is 200 to $300\times10^{-3}\,\mathrm{Vm^{-1}\,Pa^{-1}}$ for PVDF.

In most cases, the conducting covers are metal coatings. For medical applications, an optically transparent pressure transducer would, however, be preferable to measure the laser-induced acoustic signal at the same position where the tissue was irradiated. Therefore, we replaced the metal coatings by two thin layers of salt water. They are optically transparent, provide an almost perfect acoustic coupling to the tissue surface, and additionally decouple possible thermal effects caused by light absorption at the sample surface.

Thus, our transducer consists of a thin disk-shaped piece of PVDF foil (diameter of 15 mm, thickness of 25 $\mu$m), which is clamped by two brass rings used as electrodes. The brass rings form chambers that are filled with salt water (Fig. 3). The distance between the sensor foil and measuring surface (Mylar-foil) was $2.2\pm0.1$ mm.

For irradiation of the tissue, an optical parametric oscillator (OPO, GWU VisIR) pumped by the third harmonic of a Q-switched Nd-YAG laser (Quantel Brilliant B) was used. The laser system delivered 5-ns pulses at a repetition rate of 10 Hz. The OPO allowed tuning the wavelength between 400

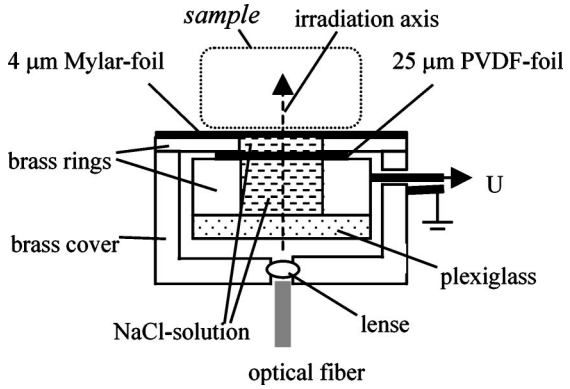


**Fig. 3** Design of the pressure transducer. A piezoelectric PVDF foil is embedded in saline water. The water cavities work at the same time as electrical capacity and as electrodes. Because PVDF is optically transparent, the transducer can be transilluminated by the laser light.

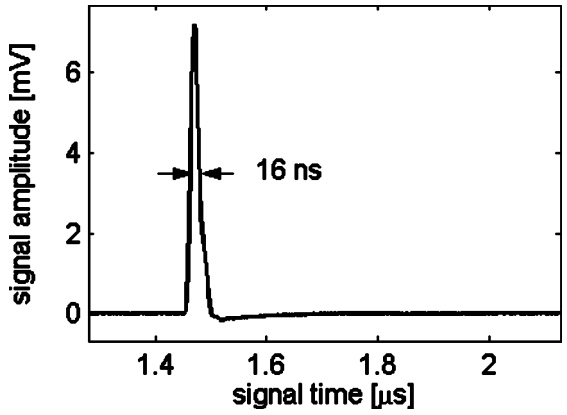


**Fig. 4** Signal generated when the irradiated light is totally absorbed by a highly absorbing dye solution in a layer thinner than 10-$\mu$m parallel to the sensor plane. The shape of the signal corresponds to the depth profile of absorption in a thin layer. The time of occurrence of the signal peak corresponds to the layer location at a depth of ~2.2 mm, and the width shows the depth resolution of about 24 $\mu$m. The signal was averaged 128 times.

and 2600 nm. The pulse energy was measured with a gentec ED-200 joule meter. The light of the OPO was guided via a 400-$\mu$m core multimode fiber to the pressure transducer and imaged onto the Mylar foil, producing a top-hat illumination with diameter of 5 mm. The pulse energy measured at the fiber output was typically 0.1 mJ. The optoacoustic voltage signal was recorded and displayed on a LeCroy 9354 AL digital oscilloscope. The chosen geometry of the setup yielded a maximum measuring depth $z_{\max}$ of 3.3 mm or a maximum measuring time of 2.2 $\mu$s (according to Fig. 2 and assuming a nonscattering sample). The maximum frequency for lamb wave excitation given by the sensor slab diameter is 0.36 MHz, corresponding to 2.7 $\mu$s. This means that regarding the maximum permissible measuring time, lamb wave excitation is neglectable.

A first set of experiments intended to show that the amplitude of the pressure signal accurately replicates the depth-resolved absorbed energy density.

If the absorption is strong and all light is absorbed within a thin sample layer parallel to the sensor surface, the signal is expected to show a narrow peak representing the narrow profile of absorption along the depth axis of the sample. The time of occurrence of this peak should correspond to the depth of the absorbing layer. We checked the behavior of the signal in such a situation with a layer of strong absorbing dye (penetration depth smaller than 10 $\mu$m) that has been put on the measuring surface of the detector.

If the absorbed light is spread over a deeper range, the signal slope mimics its depth distribution. To check this, a layer structure of two different aqueous dye solutions on top of a water layer was used. To avoid diffusion of the dye between the different layers, thin (4 $\mu$m) transparent Mylar foils were embedded at the interfaces. Such a sample can be characterized by the absorption coefficients $\mu_{a,1}$, $\mu_{a,2}$ of the dye solutions, and by the layer thickness. To simplify theoretical calculations, we considered a nonscattering medium in which the absorption coefficient $\mu_a$ varies only along the $z$ axis, and approximated our illumination by a collimated monochromatic light beam (radiant exposure $H_0$) parallel to $z$. The solution for the absorbed energy density $u(z)\,[\mathrm{J\,m^{-3}}]$ yields according to Eq. (1):

$$u(z)=\mu_a(z)\cdot\Phi(z),\quad \text{with}$$
$$\Phi(z)=H_0\cdot\exp\left[-\int_0^z dz'\ \ \mu_a(z')\right]. \tag{7}$$

Following Eq. (7), the absorbed energy density distribution in a layered sample is characterized by an exponential decay within each layer with constant absorption coefficient (Beer's law), and discontinuities at the layer interfaces. We determined the absorption coefficient of each layer from the exponential slopes in the optoacoustic signals measured at various laser wavelengths, and compared them to the absorption coefficients obtained by transmission spectroscopy.

Additionally, Eq. (7) can be used to reconstruct $\mu_a(z)$ from the absorbed energy density $u(z)$ if the radiant exposure $H_0$ is known:[10,20,25]

$$\mu_a(z)=\frac{u(z)}{H_0-\int_0^z dz'\ \ u(z')}. \tag{8}$$

We used this formula to reconstruct the depth-dependent absorption coefficient of the two layered dye samples.

In a second set of experiments, we measured the temporal behavior of a dye concentration diffusing into a gelatin sample. On top of an undoped gelatin sample, a thin film of aqueous orange-G solution was applied. Using the optoacoustic technique and the formula in Eq. (8) for reconstruction, the dye distribution was measured at various times after application, assuming that the absorption coefficient is proportional to the dye concentration in the gelatin. The results were compared with calculations based on diffusion theory. The theory predicts a depth distribution described by half of a Gaussian profile with a radius $z_0$, which grows proportional to the square root of the diffusion time:

$$\rho(z)\propto\frac{2}{\sqrt{2\pi}z_0}\cdot\exp\left(-\frac{z^2}{2z_0^2}\right), \tag{9}$$

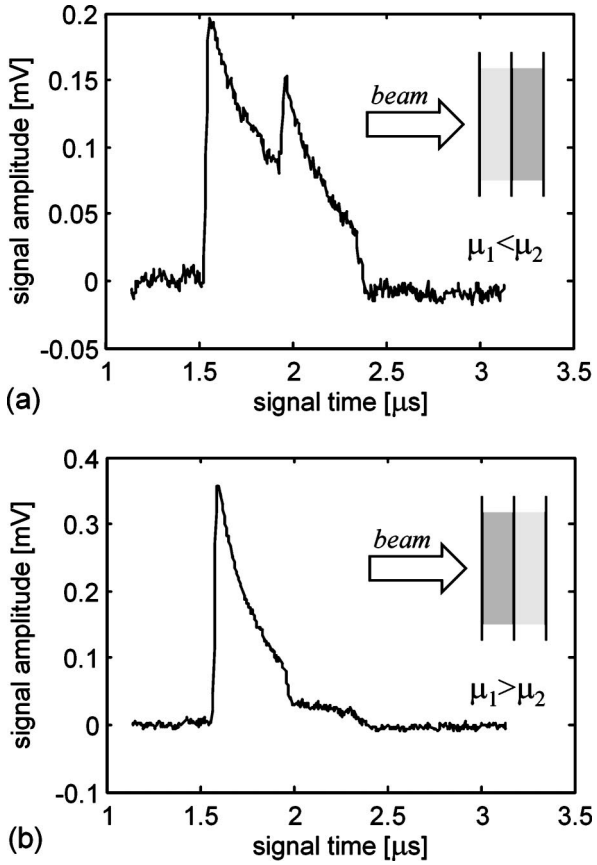


**Fig. 5** Signals obtained from layered dye samples, representing the depth profile of absorbed energy: (a) a layer with lower dye concentration followed by a layer with higher dye concentration, (b) in reverse order. The slopes represent the depth profile of absorption characterized by exponential light attenuation and by the quick change in the absorption coefficient at the layer interfaces. Apart from 128 times averaging, no other signal processing (e.g., deconvolution) was applied.

$$z_0^2 = 6Dt,$$

where $D$ is the diffusion coefficient [$m^2\,s^{-1}$].

The $(1-e^{-1})$-quantile of dye distribution (depth that has been trespassed by the $e^{-1}$ part of dye quantity) was used as definition for the penetration depth. In the case of a Gaussian distribution, the penetration depth in this definition is at $z = 0.34\,z_0$. Thus, in the diffusion model, it also grows proportional to the square root of time.

## 4 Results and Discussion

A pressure signal obtained in a situation where all light is absorbed in a thin absorbing layer (thickness smaller than 10 $\mu$m) is shown in Fig. 4. The width shows the approximate temporal resolution of our setup of about 16 ns or accordingly the depth resolution of about 24 $\mu$m. The time of occurrence (~1.47 ms) corresponds to the distance between the sensor and measuring surface (~2.2 mm).

Pressure signals obtained from the layered samples, once with the high absorbing layer on top and once in reverse order, are shown in Fig. 5. The slopes of the two peaks in the pressure signals illustrate the exponential attenuation of the

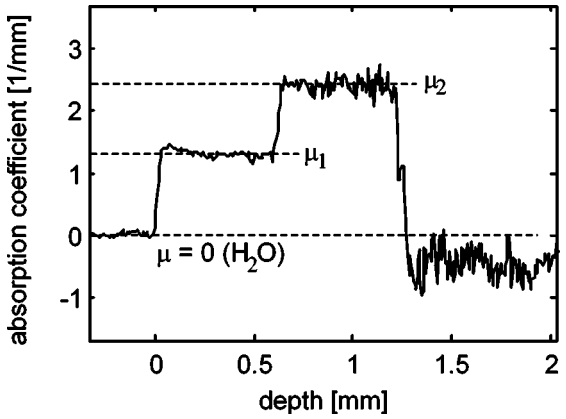


**Fig. 6** From pressure signals as shown in Fig. 5, depth profiles of the absorption coefficient $\mu_a$ can be reconstructed according to Eq. (8). In this figure, the depth profile of the sample resulting in the signal shown in Fig. 5(b) is shown. The time axis of the signal has been converted to the depth axis of the sample. The absorption coefficients are 1.30 $mm^{-1}\pm0.08$ $mm^{-1}$ in the first layer and 2.46 $mm^{-1}\pm0.14$ $mm^{-1}$ in the second layer.

irradiated light as predicted by Beer's law. The steps in the signal amplitude correspond to the fast change of absorption coefficients at the layer interfaces. The reconstruction of the sample with the weaker absorbing layer on top (Fig. 6) shows the depth profile of the absorption coefficient. The time axis of the original signal has been converted into the depth axis of the sample, considering the speed of sound and the position of the measuring surface. In each layer, the absorption coefficient remains constant, and shows a step at the interface. Figure 7 shows the comparison of optoacoustically and spectroscopically measured absorption coefficients as a function of wavelength. All three methods, the determination of the depth profile of absorption coefficient using the formula in Eq. (8), the exponential fit to the slope of the recorded pressure signal, and the spectroscopic technique show excellent agreement.

Figure 8 shows a diffusion series of optoacoustic pressure signals recorded at different times after application of the dye film on the gelatin phantom. The reconstruction of the absorp-

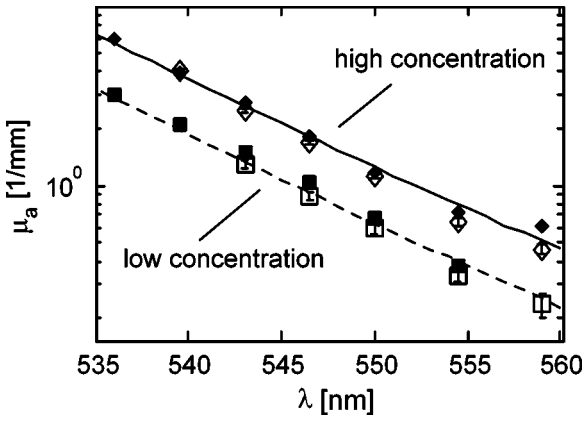


**Fig. 7** Optoacoustic measurements of $\mu_a$ for the two dye concentrations at various wavelengths by signal fitting (filled markers) and reconstruction (empty markers), compared with data obtained by transmission spectroscopy (solid and dashed line).

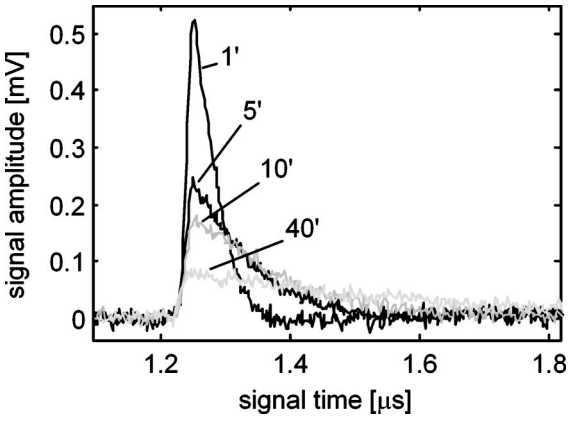


**Fig. 8** Signals from dye diffusing into a gelatin block, at various times (1, 5, 10, and 40 min) after application of a thin dye film on the gelatin surface.

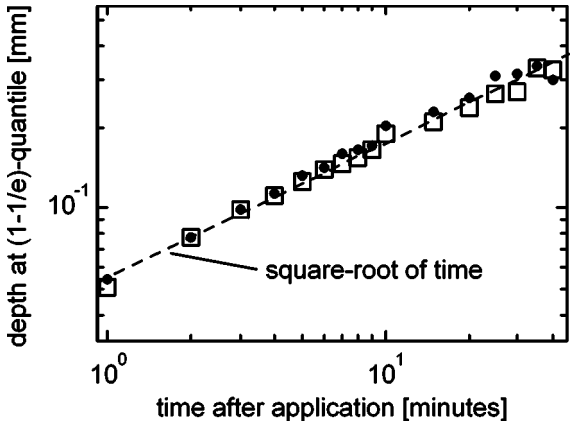


**Fig. 10** For every time after the application of the dye film, a depth can be found that has been trespassed by the $e^{-1}$ part of the dye quantity. This depth is calculated as the $1-e^{-1}$ quantile of dye distribution and used as a definition for the diffusion penetration depth. It is plotted for two diffusion series for various times after dye application, and the traces are compared with the slope expected from diffusion theory (dashed line).

tion coefficient profile using Eq. (8) is shown in Fig. 9 for two diffusion times together with Gaussian profiles calculated for comparison of the signal slope with the behavior predicted by Eq. (9). To follow the dye concentration in time, a series of OA signals was recorded. Based on such a series, the time-dependent penetration depth of the dye solution was calculated as shown in Fig. 10 for two series. The dashed line depicts the behavior described by diffusion theory (square root of time law).

These results confirm that the OA signals acquired with our detector mimic the depth profile of original pressure distribution and of the absorbed energy density. In fact, acoustic diffraction does not affect the temporal slope of the optoacoustic signal, as predicted. But still, all signals show a slight negative shift of the zero absorption line (see Figs. 4 and 5 especially), whereas the theory predicts that this base line should keep exactly the same level wherever zero absorption is reached. As stated in the theory part, the acoustic effect of the sensor foil on the signal can only be neglected for wavelengths larger than the foil thickness. This could affect the signal on a time scale in the range of the acoustic transition time of the sensor foil, which is about 10 ns, and can therefore not explain the rarefaction effect, since it occurs on a much larger time scale (some $\mu$s). Possible explanations could be searched in the field of nonlinearity and anisotropy of piezoelectric effect. Slight inverse filtering of the signals led to better results. However, we considered the unprocessed data shown to be more illustrative, and a deeper analysis of this point goes beyond the scope of this work.

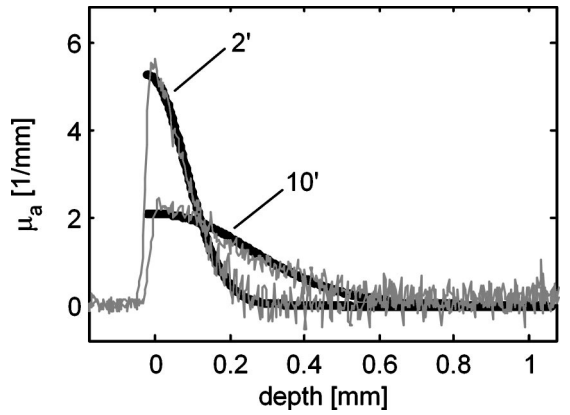


**Fig. 9** Reconstruction of absorption coefficient $\mu_a$ of a thin dye film penetrating into a gelatin block, at various times (2 and 10 min) after application, using Eq. (8). The transformed signal curves are assumed to be proportional to the depth profile of dye concentration and are shown together with Gaussian profiles (as expected from diffusion theory) for qualitative comparison.

The major two advantages of OA according to our principle are that signals can be interpreted straight forward as a replication of the absorption depth profile without the need of acoustic back projection, and that reconstruction of optical properties can be done using a simple 1-D adding-doubling algorithm.[26] This allows real-time application even with a low power computer and preserves a high amount of lucidity. The major disadvantage of methods violating the principle of near-field sensing is that for the reconstruction of a depth profile, the effect of sound diffraction has to be taken into account. This can only be done calculating the lateral distribution of absorbed energy from a model that is still incomplete, until the depth dependent optical properties of the sample are derived from the depth profile. Because only an iterative process can solve this problem, reconstruction lacks lucidity, and measuring errors can have a strong influence on the result. Additionally, it is more time consuming because illumination needs also to be calculated for the radial dimension.

Our method gives a depth profile by averaging absorption on a plane parallel to the sensor surface over the cross-sectional area of the lateral sample illumination. This defines the lateral resolution of the detector: if it is scanned over the sample surface, lateral changes on a scale smaller than the region of lateral sample illumination can hardly be detected. In the case of skin tissue, such changes include the irregularities in the interface of the papillary dermis with the epidermis, melanocytes, the vascular network, sweat glands, hair bulbs, or lateral size of pigmented moles. Instead, our method is very sensitive to depth-dependent changes of bulk absorption, in-

duced, e.g., by blood perfusion, or concentration of permeating substances, since they influence the absorption on a wide cross-sectional area. Advantage of the full potential of the method presented can be taken, if irradiation of the sample is done over a wide surface area, since this guarantees the possibility of using higher pulse energy still fulfilling radiant exposure safety standards. Consequently, the lateral resolution of our method given by the cross-sectional area of sample illumination will always be in the range of some millimeters.

## 5 Conclusions

We show that a flat pressure sensor is well suited for noninvasive depth-resolved OA measurements on layered structures. The important advantage of such a pressure transducer is that acoustic diffraction does not play any role if the sensor fulfills the transient acoustics near-field condition. Therefore, it gives real depth profiles of flat layered targets, and allows reconstruction of samples in the easiest way. Furthermore, the transducer presented is optically transparent for the exciting laser light; thus OA measurements can be done in reflection mode.

We demonstrate the use of the OA method to characterize absorption in layered samples and to monitor diffusion of absorbing substances in a tissue model.

### *Acknowledgments*

This work has been supported by the Swiss National Science Foundation (NF. 2053-066622). The authors would like to thank A. Friedrich for his help in building the transducer head and R. Nyffenegger for helpful discussions.

### *References*

1. C. Kopp and R. Niessner, ''Optoacoustic sensor head for depth profiling,'' *Appl. Phys. B: Lasers Opt.* **B68**(4), 719–725 (1999).
2. P. C. Beard and T. N. Mills, ''Characterization of post mortem tissue using time-resolved photoacoustic spectroscopy at 436, 461 and 532 nm,'' *Phys. Med. Biol.* **42**, 177–198 (1997).
3. G. Paltauf and H. Schmidt Kloiber, ''Measurement of laser-induced acoustic waves with a calibrated optical transducer,'' *J. Appl. Phys.* **82**(4), 1525–1531 (1997).
4. P. C. Beard, F. Perennes, E. Draguioti, and T. N. Mills, ''Optical fiber photoacoustic-photothermal probe,'' *Opt. Lett.* **23**(15), 1235–1237 (1998).
5. P. C. Beard and T. N. Mills, ''Extrinsic optical-fiber ultrasound sensor using a thin polymer film as a low-finesse Fabry-Perot interferometer,'' *Appl. Opt.* **35**(4), 663–675 (1996).
6. P. J. Phillips, O. T. von-Ramm, J. C. Swartz, and B. D. Guenther, ''Optical transducer for reception of ultrasonic waves,'' *J. Acoust. Soc. Am.* **93**(2), 1182–1191 (1993).
7. G. Paltauf, H. Schmidt Kloiber, and H. Guss, ''Light distribution measurements in absorbing materials by optical detection of laser-induced stress waves,'' *Appl. Phys. Lett.* **69**(11), 1526–1528 (1996).
8. G. Paltauf, H. Schmidt Kloiber, and M. Frenz, ''Photoacoustic waves excited in liquids by fiber-transmitted laser pulses,'' *J. Acoust. Soc. Am.* **104**(2), 890–897 (1998).
9. G. Paltauf, H. Schmidt Kloiber, K. P. Kostli, and M. Frenz, ''Optical method for two-dimensional ultrasonic detection,'' *Appl. Phys. Lett.* **75(8)**, 1048–1050 (1999).
10. G. Paltauf and H. Schmidt Kloiber, ''Pulsed optoacoustic characterization of layered media,'' *J. Appl. Phys.* **88**(3), 1624–1631 (2000).
11. G. Paltauf, J. A. Viator, S. A. Prahl, and S. L. Jacques, ''Iterative reconstruction algorithm for optoacoustic imaging,'' *J. Acoust. Soc. Am.* **112**(4), 1536–1544 (2002).
12. M. Frenz, G. Paltauf, and H. Schmidt Kloiber, ''Laser-generated cavitation in absorbing liquid induced by acoustic diffraction,'' *Phys. Rev. Lett.* **76**(19), 3546–3549 (1996).
13. G. Paltauf and H. Schmidt Kloiber, ''Photoacoustic cavitation in spherical and cylindrical absorbers,'' *Appl. Phys. A: Mater. Sci. Process.* **A68**(5), 525–531 (1999).
14. J. J. Niederhauser, D. Frauchiger, H. P. Weber, and M. Frenz, ''Real-time optoacoustic imaging using a Schlieren transducer,'' *Appl. Phys. Lett.* **81**(4), 571–573 (2002).
15. J. J. Niederhauser, M. Jaeger, and M. Frenz, ''Real-time three-dimensional optoacoustic imaging using an acoustic lens system,'' *Appl. Phys. Lett.* **85**(5), 846–848 (2004).
16. C. G. A. Hoelen, F. F. M. de Mul, R. Pongers, and A. Dekker, ''Three-dimensional photoacoustic imaging of blood vessels in tissue,'' *Opt. Lett.* **23**(8), 648–650 (1998).
17. K. P. Köstli, D. Frauchiger, J. Niederhauser, G. Paltauf, H. P. Weber, and M. Frenz, ''Optoacoustic imaging using a three-dimensional reconstruction algorithm,'' *JSTQE* **7**(6), 918–923 (2002).
18. X. Wang, Y. Pang, G. Ku, G. Stoica, and L. V. Wang, ''Three-dimensional laser-induced photoacoustic tomography of mouse brain with the skin and skull intact,'' *Opt. Lett.* **28**(19), 1739–1741 (2003).
19. G. Ku, X. Wang, G. Stoica, and L. V. Wang, ''Multiple-bandwidth photoacoustic tomography,'' *Phys. Med. Biol.* **49**(7), 1329–1338 (2004).
20. A. A. Karabutov, N. B. Podymova, and V. S. Letokhov, ''Time-resolved laser optoacoustic tomography of inhomogeneous media,'' *Appl. Phys. B: Lasers Opt.* **B63**(6), 545–563 (1996).
21. A. A. Oraevsky, S. L. Jacques, and F. K. Tittel, ''Measurement of tissue optical properties by time-resolved detection of laser-induced transient stress,'' *Appl. Opt.* **36**(1), 402–415 (1997).
22. A. A. Karabutov, E. V. Savateeva, N. B. Podymova, and A. A. Oraevsky, ''Backward mode detection of laser-induced wide-band ultrasonic transients with optoacoustic transducer,'' *J. Appl. Phys.* **87**(4), 2003–2014 (2000).
23. D. R. Bacon, ''Characteristics of a PVDF membrane hydrophone for use in the range 1–100 MHz,'' *IEEE Trans. Sonics Ultrason.* **SU-29**(1), 18–25 (1982).
24. H. Schoeffmann, H. Schmidt-Kloiber, and E. Reichel, ''Time-resolved investigations of laser-induced shock waves in water by use of polyvinylidenefluoride hydrophones,'' *J. Appl. Phys.* **63**(1), 46–51 (1988).
25. A. A. Karabutov and A. P. Kubyshkin, ''New contactless method for recording surface acoustic waves,'' *Moscow Univ. Phys. Bull.* **50**(6), 25–28 (1995).
26. S. A. Prahl, J. C. van-Gemert, and A. J. Welch, ''Determining the optical properties of turbid media by using the adding-doubling method,'' *Appl. Opt.* **32**(4), 559–568 (1993).